$LiPF_6$ Studied With the New TA Instruments™ TGA Smart-Seal™ Pans

Keywords: TGA Smart-Seal Pan, batteries, glovebox, inert

TA491

ABSTRACT

Atmospheric-sensitive samples pose special challenges to researchers. To ensure sample integrity, protection against contact with moisture and atmospheric gases must be secured across the entire analytical workflow. Battery materials are representative of systems containing substances that are highly sensitive to atmospheric contamination. For example, lithium hexafluorophosphate ($LiPF_6$), the most common salt used in Li-ion batteries, is especially sensitive to water contamination. Thermogravimetric analysis (TGA) of atmospheric-sensitive samples presents unique difficulties, as the sample must be in an open container when analyzed so that gases can evolve freely. Standard TGA sealed pans offered by manufacturers often fail to protect the most sensitive samples as they are opened and exposed to the ambient atmosphere prior to loading. Therefore, TA Instruments has developed the TGA Smart-Seal Pan, which opens autonomously in the TGA furnace based on temperature. This application note presents data on the TGA analysis of $LiPF_6$ using the TGA Smart-Seal Pans.

INTRODUCTION

Performing experimental studies on highly atmospheric-sensitive samples is challenging. Materials that are sensitive to atmospheric contamination often require both the sample preparation and the analysis to be performed in a glovebox. Installation and use of analytical instrumentation in a glovebox can be cumbersome and counterproductive [1]. To help eliminate the necessity of operating a TGA in a glovebox, TA Instruments has developed the TGA Smart-Seal Pan (Figure 1). Nitinol shape-memory technology is used to autonomously open a hermetically sealed TGA pan in the TGA furnace based on temperature. With these pans, atmospherically-sensitive samples can be analyzed with the TGA placed in ambient conditions, without compromising the sample integrity. Pan details and an examination of the hermetic seal quality have been reported elsewhere [1].

Lithium hexafluorophosphate ($LiPF_6$) is highly hygroscopic and the most common electrolyte salt used in lithium-ion batteries [2,3]. Under dry conditions, the neat salt decomposes in a single step to lithium fluoride (LiF) and phosphorous pentafluoride (PF_5) between 150 – 250 °C. Under wet conditions, it can produce both hydrogen fluoride (HF) and phosphoryl fluoride (POF_3) along two separate decomposition paths [3,4]. Figure 2 details the chemical decomposition pathways. The wet decompositions occur at low temperature relative to the decomposition of the dry salt.

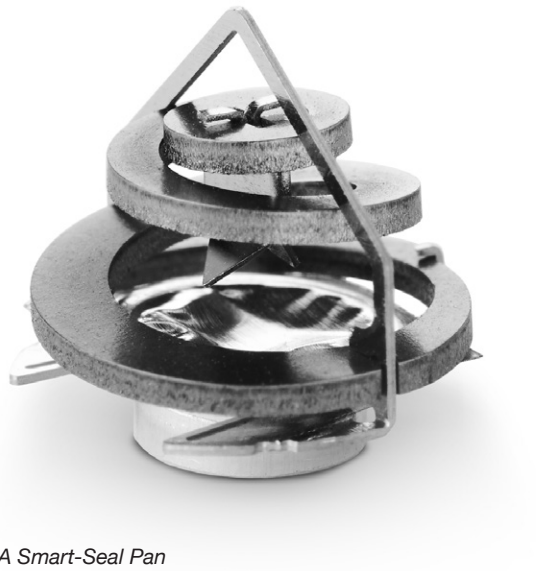

Figure 1. TGA Smart-Seal Pan

Dry $LiPF_6 \rightarrow LiF + PF_5$

Wet $LiPF_6 + H_2O \rightarrow LiF + POF_3 + 2HF$

$PF_5 + H_2O \rightarrow POF_3 + 2HF$

Figure 2. $LiPF_6$ decomposition pathways

There have been numerous papers published in the literature using thermogravimetry to study dry and wet $LiPF_6$ powder [3-7]. In two studies, the $LiPF_6$ was exposed to controlled levels of water vapor by mixing it into the purge gas stream [3,4]. In this setup, the sample interacts with water during the entire decomposition. In other work, the $LiPF_6$ was deliberately exposed to atmospheric levels of water vapor for specific time periods [5,6]. After exposure, the sample decomposition takes place within the TGA in an inert environment. The latter approach is the one adopted here as it more closely mimics the potential exposure a sample contained within a traditional sealed TGA pan will experience upon opening.

EXPERIMENTAL

The tests reported here were performed with battery-grade (≥ 99.99%, trace metals basis) $LiPF_6$ purchased from Sigma Aldrich Co. Upon receiving, the sample was stored in a glovebox environment for which the measured water vapor level was < 0.5 ppm and the measured oxygen level was < 0.1 ppm.

Two Discovery™ 5500 TGA instruments were used in this study. One operated under ambient conditions, while the other was installed in a glovebox under a nitrogen atmosphere. Samples for both TGAs were sealed and run in TGA Smart-Seal Pans to make data comparisons straightforward. Sample amounts of between 4-6 mg were sealed in the TGA Smart-Seal Pans and ramped at 10 °C/min to 600 °C. Once the sample was loaded, the ambient TGA furnace was flushed with five 9's nitrogen for 20 minutes to obtain a highly inert atmosphere. Previous work has shown that inert levels of less than 50 ppm of oxygen and water vapor, as measured by external sensors, can be obtained by this procedure.

A Nicolet™ iS50 FTIR Spectrometer with a zero-gravity IR cell from RedShift srl was connected to the outlet of the ambient TGA instrument. The transfer line was heated to 200 °C. The scan configuration was eight scans at a resolution of four.

RESULTS AND DISCUSSION

The data is presented in two sections: one for TGA and one for FTIR. The results presented will clearly show that the $LiPF_6$ run in the TGA Smart-Seal Pan within the ambient TGA remained dry, or did not experience further contamination if priorly exposed to water vapor, during the experiment's execution.

TGA Data

This section describes the TGA data collected on $LiPF_6$. Figure 3 below shows a run of dry $LiPF_6$ with a TGA installed in a glovebox. The data, including the derivative which can pick up small features, indicate that the sample decomposes in a single weight loss step of approximately 82.4%. The peak in the weight loss occurs near 220 °C. This is consistent with other published TGA data of anhydrous $LiPF_6$ [3-6].

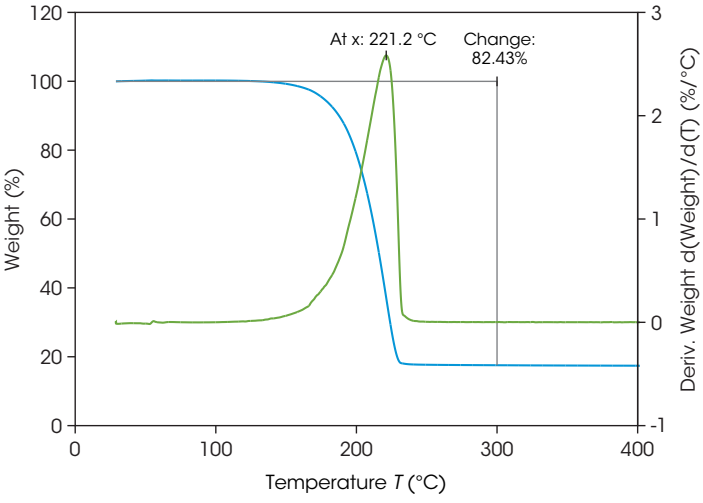

Figure 3. $LiPF_6$ TGA data collected with glovebox TGA

Figure 4 shows an overlay of a dry run with two runs in which the $LiPF_6$ was exposed to ambient levels of water vapor for approximately 30 seconds and 5 seconds. The exposure was done in the following manner. The sample was loaded into the open pan in the glovebox. It was then brought through the glovebox antechamber, exposed to atmospheric conditions for the specified amount of time, and then reintroduced back into the glovebox. Before reintroduction, the antechamber was cycled between vacuum and inert gas three times. The samples were then sealed and run in the TGA within the glovebox. The data now shows a second, earlier, weight loss event. The weight losses for the 5 and 30 second exposures are 2.3% and 4.3%, respectively, thus demonstrating growth with increased exposure time. These weight losses occur between 70 °C to 75 °C.

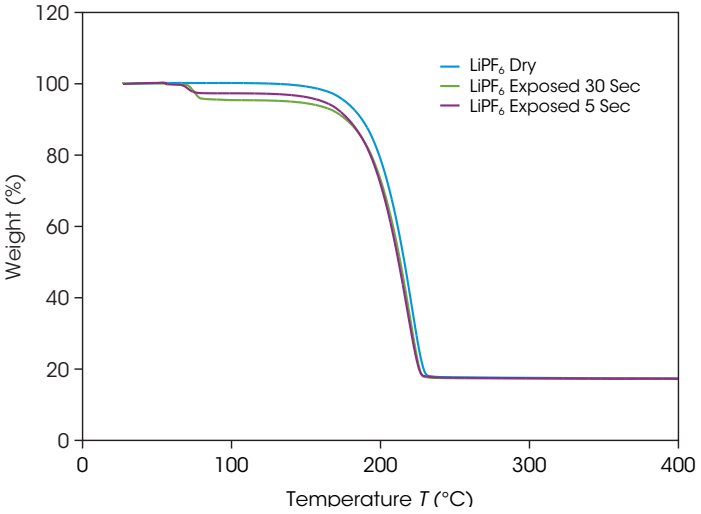

Figure 4. Overlay TGA data of $LiPF_6$ exposed to ambient moisture levels for varying amounts of time

A very similar weight loss has also been observed in published data, though it has been attributed to either water in the crystal structure [5,6], or removal of the free acid, HF, that can sometimes remain depending upon the production process [7]. As will be shown, FTIR data of this weight loss event point here to this being associated with the neat $LiPF_6$ wet decomposition pathway in Figure 2. In any case, its presence is a marker of sample contamination.

A 30 second exposure simulates the time required to load a TGA sample. Therefore, it is of the order of time a sample might be exposed to the atmosphere when using a traditional sealed TGA pan. Clearly, $LiPF_6$ is reactive enough with water vapor that even an exposure of only 5 seconds will contaminate the sample and influence the data.

Figure 5 below shows a run of $LiPF_6$ in a TGA Smart-Seal Pan in the ambient TGA. The sample was sealed in the glovebox and then transferred to the ambient TGA and run immediately. Again, a single weight loss event is detected of size 83.3% and the peak position once more is near 220 °C. No indication of a weight loss around 70 °C is detected (the small feature in the derivative is due to the opening of the TGA Smart-Seal Pan). Figure 6 shows

excellent agreement between an overlay of this data with the dry run in the glovebox. The TGA data, along with the FTIR data below, confirms the TGA Smart-Seal Pan to have kept the sample dry in transport from the glovebox, during loading, and experiment execution within the ambient TGA.

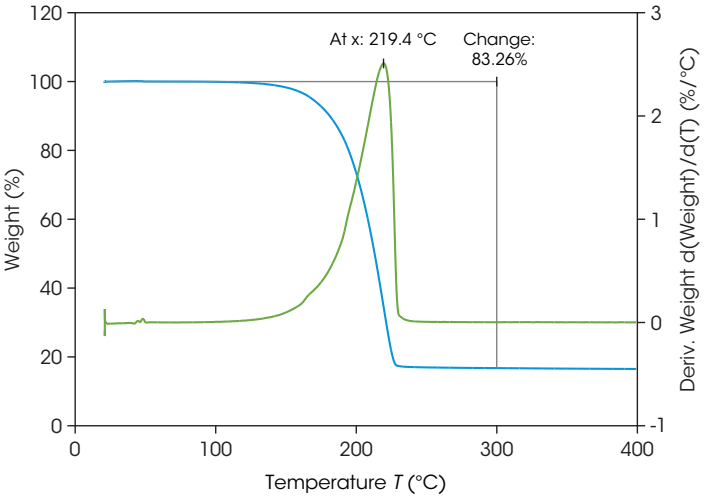

Figure 5. $LiPF_6$ TGA data collected with ambient TGA

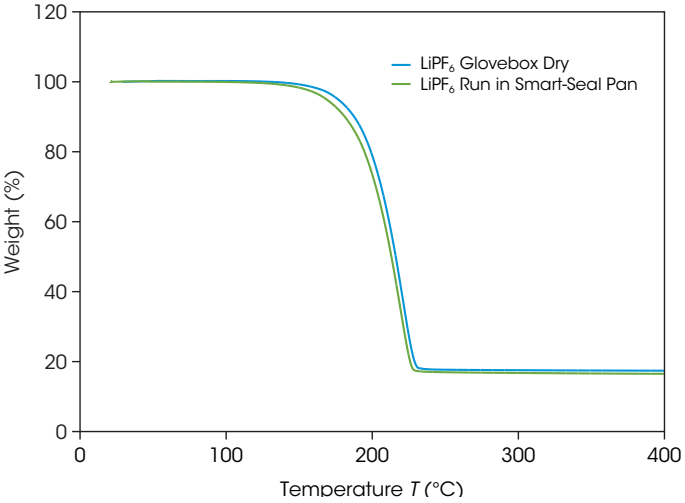

Figure 6. Overlay $LiPF_6$ glovebox and ambient TGA data

Finally, Figure 7 shows an overlay of the data from Figure 5 plus data from additional $LiPF_6$ samples which remained on the autosampler tray for 24 and 48 hours. All samples were prepared identically in the glovebox before transfer to the TGA autosampler. As with the data in Figure 5, no indication of any earlier weight loss is detected. The data presented here indicates that the seal on the TGA Smart-Seal Pan is excellent and can protect the $LiPF_6$ material for up to 48 hours. With a 25 position autosampler, running 25 samples at 10 °C/min to 600 °C and including cool down and sample load / unload times, total experiment time would be less than 48 hours. Previous data using desiccant water vapor sensitive samples have indicated the seal can protect samples for up to two weeks [1].

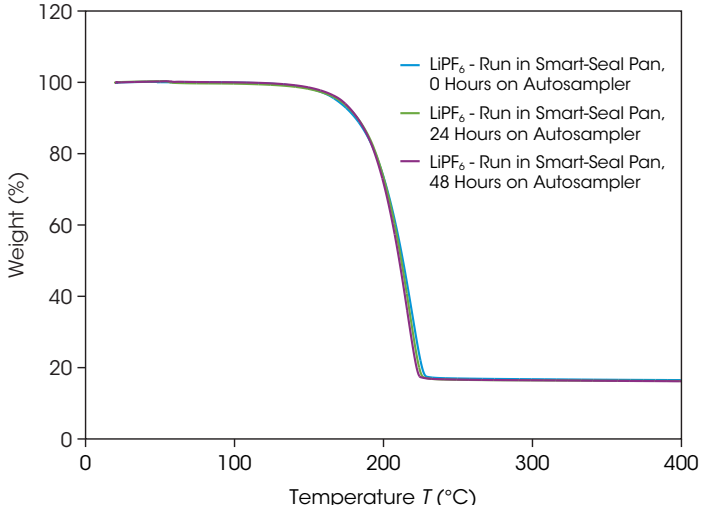

Figure 7. Overlay $LiPF_6$ TGA data from samples sitting on the autosampler for 0, 24, and 48 hours

FTIR Data

In addition to TGA data, in-situ FTIR data on the evolved gasses was also collected. One distinct advantage that ambient TGAs have over glovebox TGAs is a much easier connection to spectrometers. With a TGA installed in a glovebox, either the spectrometer must also be similarly installed, or the transfer line must pass through the glovebox wall to an exterior spectrometer. In the former case, even more valuable glovebox space is taken, and in the latter, installations are difficult and are potentially costly.

Figure 8 shows the Gram-Schmidt curve of total IR intensity for the TGA data from Figure 5. A single peak is detected, consistent with the single weight loss event captured by the TGA. Expanding the data does not show any other structure. Figure 9 shows the IR spectrum from the peak in the Gram-Schmidt plot. This spectrum matches that of phosphorous pentafluoride (PF_5) [3]. Between 3600 and 4400 cm^{-1} there is some small detection of hydrogen fluoride (HF), and at 1400 cm^{-1} there is some small detection of phosphoryl fluoride (POF_3). Both are likely by-products resulting from the interaction of evolved PF_5 with small concentrations of water vapor (< 50 ppm) in the furnace or within the FTIR gas cell. This logically follows from the fact that the relative intensities of the HF and POF_3, as compared to the PF_5, never changed across the 0, 24, and 48 hour long experiments with the ambient TGA.

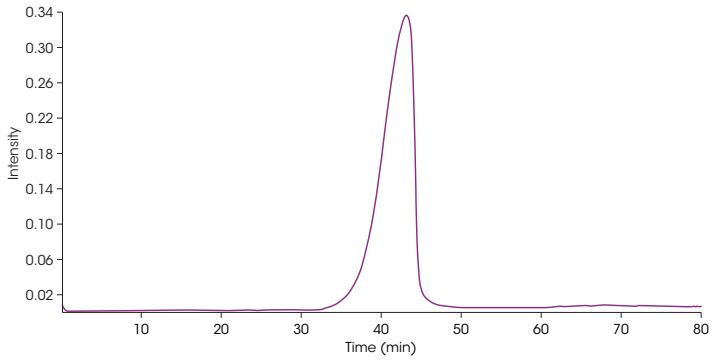

Figure 8. Gram-Schmidt plot from TGA data in Figure 3

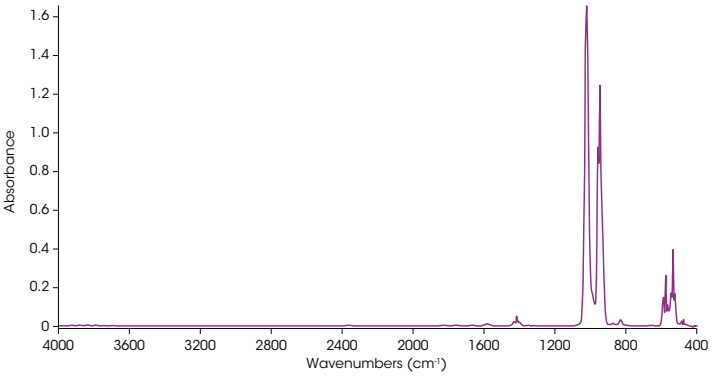

Figure 9. IR spectrum from the peak in the Gram-Schmidt plot in Figure 8

Figures 10 and 11 show overlays of the Gram-Schmidt plots and the peak spectra for the TGA data from Figure 7. In all three cases, only a single peak occurs in the Gram-Schmidt and the spectrum is that of PF_5.

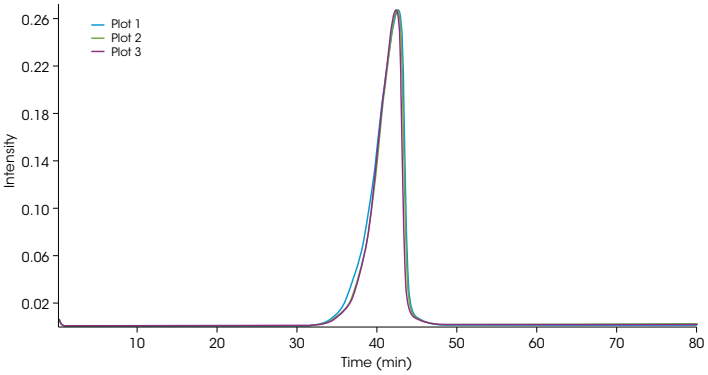

Figure 10. Overlay of Gram-Schmidt plots from the data in Figure 7

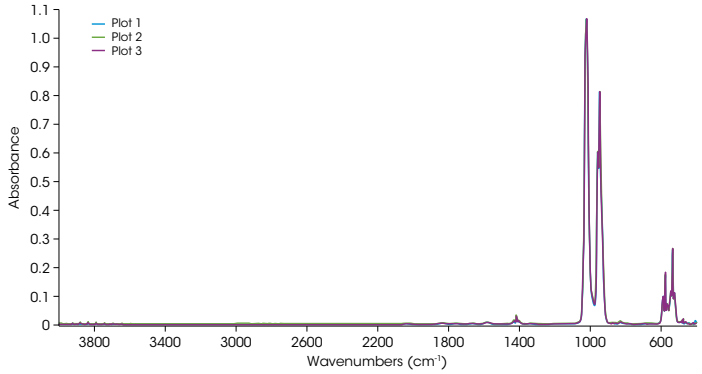

Figure 11. Overlay of spectra from peaks in Gram-Schmidt plot of Figure 10

Figure 12 shows the Gram-Schmidt plot from data of a $LiPF_6$ sample exposed to ambient conditions for 30 seconds in the manner outlined previously. The data now has two peaks. The smaller one is new and correlates with the small weight loss seen in the TGA data below 100 °C.

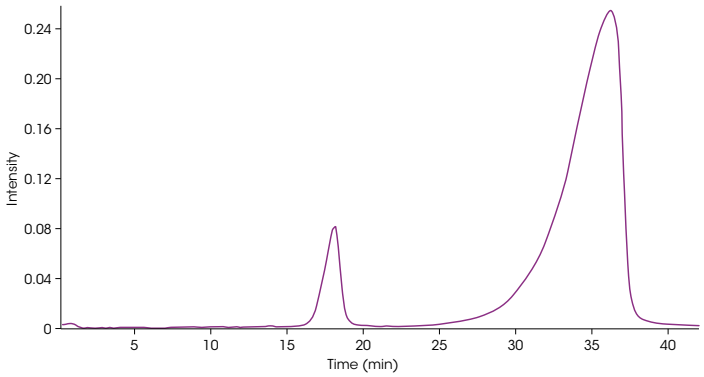

Figure 12. Gram-Schmidt plot for $LiPF_6$ sample exposed to ambient conditions for 30 seconds

Figures 13 and 14 show spectra from peaks one and two, respectively. The spectrum in Figure 14 corresponding to the second peak in the Gram-Schmidt plot and the weight loss centered at 220 °C in the TGA data, is exactly that of PF_5 as can be seen by comparing to Figure 9. The spectrum in Figure 13 corresponding to the first peak in the Gram-Schmidt plot and the weight loss under 100 °C in the TGA data, is that of HF and POF_3 combined [3]. Exposure of $LiPF_6$ to atmospheric levels of water vapor, as can happen when opening a standard TGA sealed pan followed by loading into the TGA furnace and heating, leads to a reaction between the $LiPF_6$ as detailed in Figure 2. The TGA data is affected by the appearance of a second, lower temperature, weight loss event, and the FTIR identifies the gases evolving as HF and POF_3.

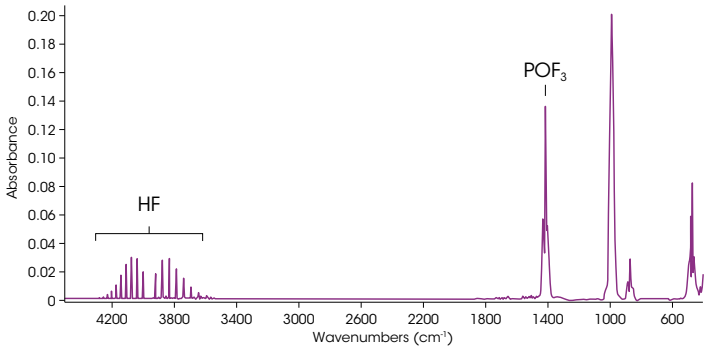

Figure 13. Spectrum from first peak in Gram-Schmidt plot shown in Figure 12

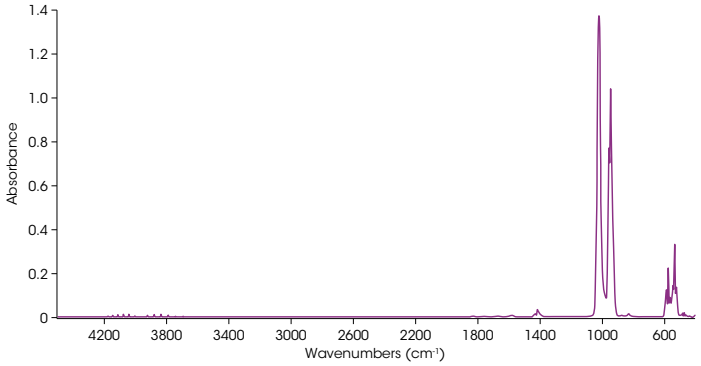

Figure 14. Spectrum from second peak in Gram-Schmidt plot shown in Figure 12

Figure 4 shows how the TGA weight loss event below 100 °C appears and then grows larger as the exposure time to water vapor increases. Figure 15 shows the same for the FTIR data. In this overlay, data from samples exposed for 5, 30, 60, and 150 seconds is shown. Clearly, the amount of HF and POF_3 increases with increasing exposure and thus the weight loss occurring under 100 °C is a result of the interaction of the neat $LiPF_6$ powder with atmospheric water vapor.

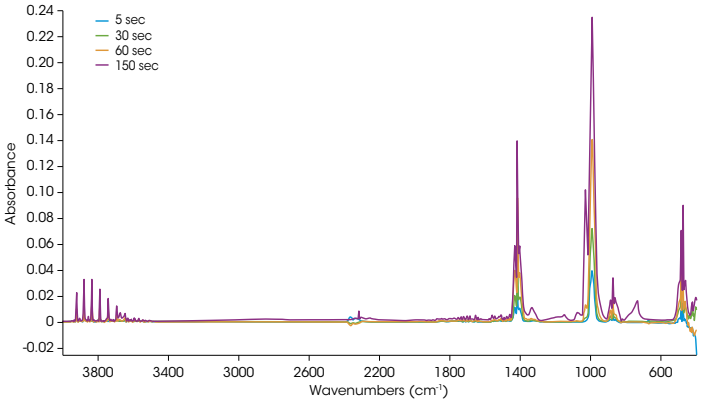

Figure 15. Overlay of FTIR data for $LiPF_6$ exposed to ambient atmosphere for 5, 30, 60, and 150 seconds

CONCLUSION

In this application note, $LiPF_6$ was studied using TGA and FTIR. The TGA data was a comparison between a TGA installed in a glovebox and one installed in ambient conditions. Since $LiPF_6$ is highly sensitive to water vapor, and must be studied under inert conditions, the comparison provides information on the performance of the TGA Smart-Seal Pans and the inert conditions of the furnace. The performance of both was shown to be excellent with no indication of water vapor contamination of the $LiPF_6$ resulting from transport from the glovebox or sitting on the autosampler for up to 48 hours. FTIR data collected on samples run in the ambient TGA confirm this conclusion. A second, low temperature weight loss appears in the TGA data of water vapor contaminated samples, and FTIR data indicates that the gases evolved are HF and POF_3. This is consistent with the degradation of neat $LiPF_6$ after exposure to water vapor.

REFERENCES

1. C. G. Slough, Introducing the TGA Smart-Seal Pan: A Self-Opening Thermogravimetric Sample Pan, TA Instruments application note, TB104, 2024.

2. J. Y. Han and S. Jung, Thermal stability and the effect of water on hydrogen fluoride generation in lithium-ion battery electrolytes containing $LiPF_6$, Batteries, **8**, 61, 2022.

3. H. Yang, G. V. Zhuang, and P. N. Ross Jr., Thermal stability of $LiPF_6$ salt and Li-ion battery electrolytes containing $LiPF_6$, J. of Pwr Srcs, **161**, pp 573-579, 2006.

4. S. Solchenbach, M. Metzger, M. Egawa, H. Beyer, and H. A. Gasteiger, Quantification of PF_5 and POF_3 from side reactions of $LiPF_6$ in Li-ion batteries, J. of Electchem.Soc., **165**, (13) PP AA3022 – AA3028, 2018.

5. L. D. Kock, M. D. S. Lekgoathi, P. L. Crouse, and B. M. Vilakazi. Solid state vibrational spectroscopy of anhydrous lithium hexafluorophosphate ($LiPF_6$) J. Mol. Struct. **1026**, pp. 145-149, 2012.

6. M. D. S. Lekgoathi, B. M. Vilakazi, J. B. Wagener, J. P. Le Roux, and D. Moolman, Decomposition kinetics of anhydrous and moisture exposed $LiPF_6$ salts by thermogravimetry, J. Fluorine Chem., **149**, pp. 53-56, 2013.

7. L. Jian-wen, L. Xin-hai, W. Zhi-xing, G. Hua-jun, P. Wen-jie, Z. Yun-he and H. Qi-yang, Preparation and characterization of lithium hexafluorophosphate for lithiu-ion battery electrolyte, Trans. Nonferrous Met.Soc. China, **20**, pp 344-348, 2010.

ACKNOWLEDGEMENTS

For more information or to request a product quote, please visit www.tainstruments.com to locate your local sales office information.

This paper was written by Gray Slough, PhD at TA Instruments.